

Supporting Information

Postsynthetic Ionization of Imidazole-Containing Metal-Organic Framework for Cycloaddition of Carbon Dioxide and Epoxides

Jun Liang,^{ab} Rui-Ping Chen,^a Xiu-Yun Wang,^a Tao-Tao Liu,^a Xu-Sheng Wang,^a Yuan-Biao Huang,^{*a} and Rong Cao^{*ab}

^a State Key Laboratory of Structural Chemistry, Fujian Institute of Research on the Structure of Matter University of Chinese Academy of Sciences Fujian, Fuzhou, 350002, P.R. China
rcao@fjirsm.ac.cn. Fax: (+86) 591-8379-6710;

^b Department of Chemistry, College of Chemistry and Chemical Engineering, Xiamen University Xiamen 361005, P. R. China

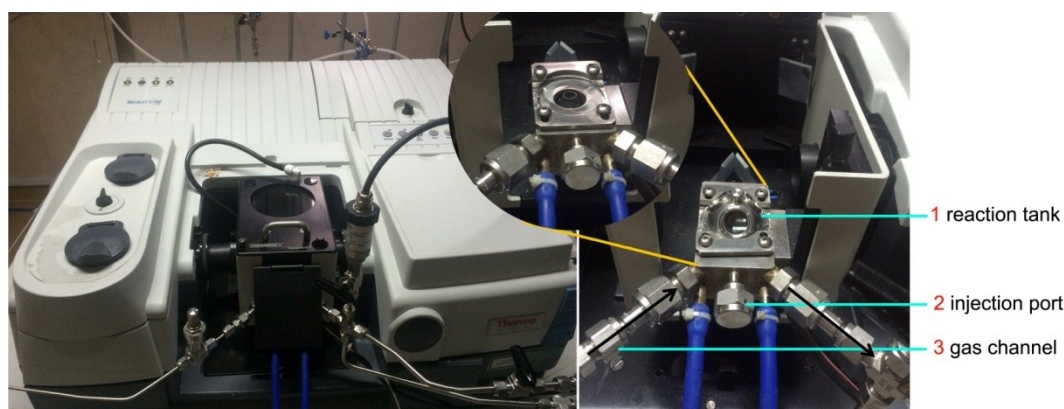
1. General experiments

2-(imidazol-1-yl)terephthalic acid (Im-H₂BDC·HCl) was prepared by a similar process according to the literature.¹ Other reagents were purchased from commercial sources and used as received. N₂ and CO₂ sorption isotherms of Im-UiO-66 (**1**) and (I-)Meim-UiO-66 (**2**) were measured by using a Micrometrics ASAP 2420 instrument at 77 K and 273K, 298 K, respectively. Before the measurement, the samples were evacuated and activated at 393 K in vacuum for 10 h. Adsorption enthalpies for CO₂ of **1** and **2** were calculated by virial method in Origin software. Powder X-ray diffraction patterns (PXRD) were recorded on a Rigaku Dmax 2500 diffractometer equipped with Cu-K α radiation ($\lambda = 1.54056 \text{ \AA}$) over the 2θ range of 5–45° with a scan speed of 3° min⁻¹ at room temperature. Thermogravimetric analyses (TGA) were performed under a nitrogen atmosphere with a heating rate of 10°C min⁻¹ by using an SDT Q600 thermogravimetric analyser. The samples were activated at 393 K in vacuum for 10 h before TGA test. Infrared (IR) spectra were recorded using KBr pellets on a PerkinElmer Spectrum One in the range of 400–4000 cm⁻¹. Elemental analyses of C, H, and N were carried out on an Elementar Vario EL III analyzer. The ¹H NMR was performed at AVANCE III Bruker Biospin spectrometer, operating at 400 MHz. About 6 mg Zr-MOF samples was dissolved in 500 μ l DMSO-*d*₆ and then 30 μ L HF was added. The morphologies of MOF nanoparticles were studied using a FEIT 20 transmission electron microscope (TEM) working at 200 kV and scanning electron microscope (SEM) working at 10 KV. The gas chromatography (GC)

measurements were performed on a G7890A-GC. The gas chromatography–mass spectrometry (GC-MS) measurements were performed on a Varian 450-GC/240-MS. Temperature-programmed desorption (TPD) profiles of CO₂ and NH₃ from the MOFs were conducted on an AutoChem 2920 equipped with a TCD detector as follows. For CO₂-TPD: A sample of 100 mg was pretreated in Ar at 373 K for 2 h. After cooled to 323 K, the sample was exposed to CO₂ (99.99%, China) for 60 min and then purged with Ar at 373 K to remove physical adsorbed CO₂ and then cooled down to 323 K. CO₂-TPD was measured from 323 to 564 K in a Ar flow at a rate of 5 °C/min. For NH₃-TPD: A sample of 50 mg was pretreated in Ar at 373 K for 2 h. After cooled to 323 K, the sample was exposed to 1.01% NH₃/Ar for 30 min, followed by flushing with Ar at 373 K to remove physical adsorbed ammonia, and then cooled down to 323 K. NH₃-TPD was measured from 323 to 673 K in a Ar flow at a rate of 5 °C/min.

In situ FT-IR spectra measurements:

In situ FT-IR spectra of (I)Meim-Uio-66 catalyzed cycloaddition of epoxide with CO₂ was qualitatively conducted on a NICOLET 6700 instrument at 373K (Scheme S1). Before the measurement, the catalyst was evacuated and activated at 393 K in vacuum for 6 h. Firstly, about 30 mg of (I)Meim-Uio-66 was filled in the reaction tank before vacuum treatment for a few minutes to set the signal of catalyst as the signal background, then the reaction tank was set at 0.1 MPa CO₂ atmosphere. Pure N₂ was used to dilute the CO₂ until suitable stable signal strength of CO₂ was detected. After that, 0.1 ml epichlorohydrin was injected into the closed tank before heating up to 373K while conducting real time monitoring the signals.



Scheme S1. Schematic view of NICOLET 6700 instrument for *in situ* FT-IR spectra measurement.

Typical catalytic reaction procedure:

In a typical catalytic cycloaddition, 10 mmol substrate and catalyst (0.05 g, 0.745 mol%, according to the amount of imidazolium) were placed in a 15 mL thick-walled reaction tube equipped with a magnetic stirrer. After being sealed, the autoclave was carefully flushed once with CO₂. The reaction was carried out at specified temperature and 0.1 MPa CO₂ pressure for a desired period of time. The qualitative analysis of product was determined by GC-MS and quantitative analysis by GC. The catalytic reaction procedure of epichlorohydrin: 50 mg of catalyst and 10 mmol epichlorohydrin were placed in a 15 mL thick-walled reaction tube equipped with a magnetic stirrer. After being sealed, the autoclave was carefully flushed once with CO₂. The reaction was carried out at 120 °C for 24 h and 0.1 MPa CO₂ atmosphere. The qualitative analysis of product was determined by GC-MS and quantitative analysis by GC. The recyclability test was conducted as follows: after reaction, **2** was separated by centrifugation and washed by ethyl acetate twice. After being dried in vacuum, it can be directly used in next catalytic reaction.”

2. Syntheses

Synthesis of 2-(imidazol-1-yl)terephthalic acid (Im-H₂BDC·HCl·H₂O)

A mixture of K₂CO₃ (1.934 g, 0.014 mol), 2-bromobenzoic acid (1.225 g, 0.005 mol), imidazole (1.71 g, 0.025 mol), CuSO₄·5H₂O (0.050 g, 0.2 mmol) were ground sufficiently in an agate mortar. Then, the mixture was transferred into a 15 mL Teflon-lined autoclave, which was sealed and heated at 210°C for 10 h under N₂ atmosphere. After cooling the reaction system to room temperature, the reaction mixture was dissolved in 60 ml water, and then filtered off. The filtrate was adjusted with 6 M dilute hydrochloric acid to pH 2.0–3.0 and filtered to obtain gray precipitate. Recrystallization from dilute hydrochloric acid yielded colourless rod crystals of im-H₂BDC·HCl·H₂O. ¹H NMR (DMSO-*d*₆, 25°C): δ = 7.85 (s, 1H, N-CH-CH-N), 8.04 (s, 1H, N-CH-CH-N), 8.20-8.28 (br, 3H, Ar-H), 9.49 (s, H, N-CH-N); ¹³C NMR (DMSO-*d*₆, 25): 165.4, 164.6, 136.8, 135.1, 134.6, 132.0, 131.4, 131.2, 129.1, 123.9, 119.5.

Synthesis of Im-UiO-66 (1)

A mixture of ZrCl_4 (47 mg, 0.2 mmol), $\text{Im-H}_2\text{BDC}\cdot\text{HCl}\cdot\text{H}_2\text{O}$ (57 mg, 0.2 mmol) and acetic acid (1.2 g) in 5 mL DMF was sonicated for 5 minutes and then transferred into autoclaves. The tightly capped autoclave was kept in an oven at 120 °C for 48 h under static conditions before cooling slowly to room temperature in 10 hours. The precipitates were isolated by centrifugation and washed with 5 mL of DMF three times and followed by washing with 6 mL of methanol two times. After drying under vacuum for 30 minutes, each 1g crystals product was washed with 100 mL of methanol four times. During each wash, the suspension was kept at room temperature for 12 h before being centrifuged. Finally, the solids were dried at 120 °C under vacuum. We have tried our best to grow large single crystals by tuning the reactant ratios and mixture concentrations, however, unfortunately, no single crystal suitable for more detailed structure analysis was obtained. The established condition conveniently led to small nanoparticles of Im-UiO-66 (**1**) in the absence of any additional chemicals. IR characteristics (KBr, ν_{max} , cm^{-1}): 3426 (w), 3145 (w), 1598 (s), 1503 (s), 1427 (s), 1377 (m), 773 (s), 657 (s).

Synthesis of (I)Meim-UiO-66 (2)

A CH_3CN (15 mL) suspension of **1** (0.346 g) and methyl iodide (0.5 ml) was heated at 80°C for 48 h under N_2 atmosphere. The product was collected by centrifugation washed with CH_3CN (10 mL \times 2), MeOH (10 mL \times 2), Ether (10 mL \times 2) to generate (I)Meim-UiO-66 as yellow powder solids after drying at 60 °C under vacuum for 12h. Elemental analysis for **2** (found): C, 30.1; N, 5.56; H, 3.69; Zr, 18.1 (%). IR characteristics (KBr, ν_{max} , cm^{-1}): 3436 (w), 2962 (s, CH_3), 1718 (s), 1599 (s), 1424 (s), 1384 (m), 1261(s), 1090 (m), 804 (s), 658 (m).

Synthesis of 1 (NS) and 2 (NS)

$\text{Im-H}_2\text{BDC}\cdot\text{HCl}\cdot\text{H}_2\text{O}$ (57 mg), $\text{Zr}(\text{NO}_3)_4\cdot 5\text{H}_2\text{O}$ (86 mg) and acetic acid (2 ml) were successively added into 3 ml DMF and the mixture was sonicated sufficiently before being transferred into autoclaves. The tightly capped autoclave was kept in an oven at 120 °C for 48 h under static conditions before cooling slowly to room temperature in 10 hours. The precipitates were isolated by centrifugation and washed with 5 mL of DMF two times and followed by washing with 6 mL of methanol two times. The solvent exchange process was the same as that of Im-UiO-66 (**1**). The synthesis of **2**

(NS) was the same as that of **2**. Elemental analysis for **2** (NS) (found): C, 26.7; N, 5.0; H, 3.4; Zr, 20.2 (%).

3. Characterizations

Single Crystal X-ray Diffraction Studies of Im-H₂BDC

For the single crystal analysis of im-H₂BDC, a colorless block crystal was taken directly from the mother liquor, transferred onto a loop. The crystal was kept at 100.00(10) K during data collection on a supernova diffractometer equipped a Multilayers mirror Cu-K α radiation ($\lambda = 1.5418 \text{ \AA}$) by using a ω scan mode. The crystal structure was solved by direct method and refined by full-matrix least squares on F² using ShelXL package. Non-hydrogen atoms were refined with anisotropic displacement parameters. Crystallographic data for the structures reported in this paper have been deposited in the Cambridge Crystallographic Data Center with CCDC reference number 1499016.

The structural analysis of Im-H₂BDC·HCl·H₂O

As shown in Fig. S1, the dihedral angle between imidazole (im) group and the plane where H₂BDC backbone lies is 69.6°. It is notable that the existence of imidazole group doesn't affect the adjacent carboxyl group significantly, as two carboxyl groups are almost in the same plane with benzene core. These features are necessary and provide the essential structural information for the formation of targeted **fcu** Zr-based MOF, Im-UiO-66 (Fig. S5).

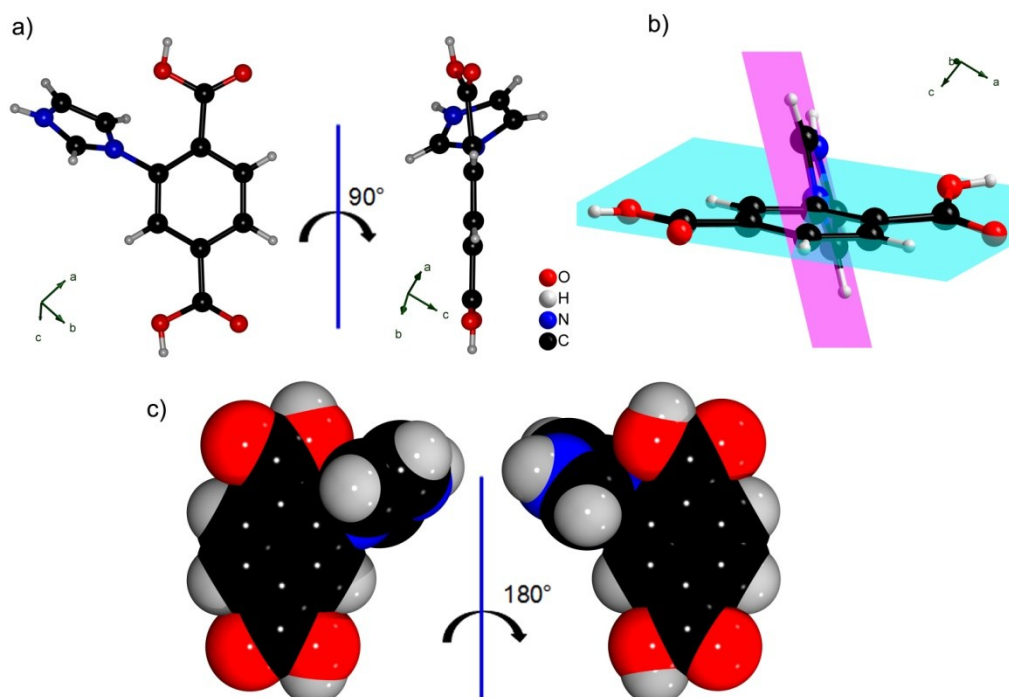


Fig. S1 (a) and (b) Ball and stick and (c) space-filling views of Him-H₂BDC (Cl atom is omitted).

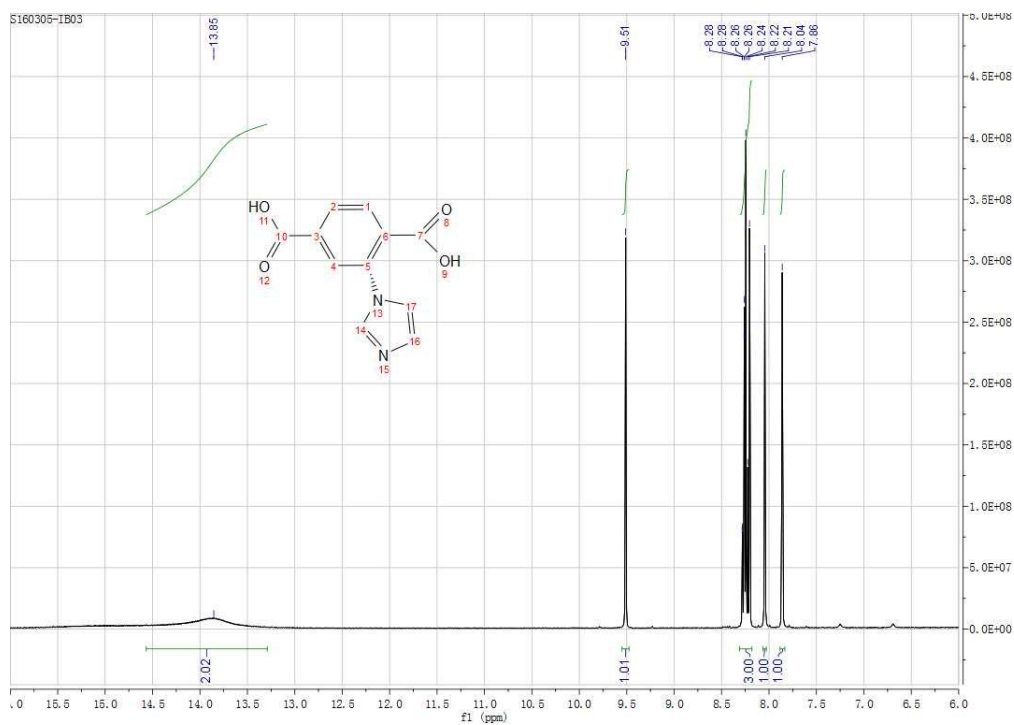


Fig. S2 ¹H NMR spectrum of Im-H₂BDC·HCl·H₂O in DMSO-*d*₆ (r.t.).

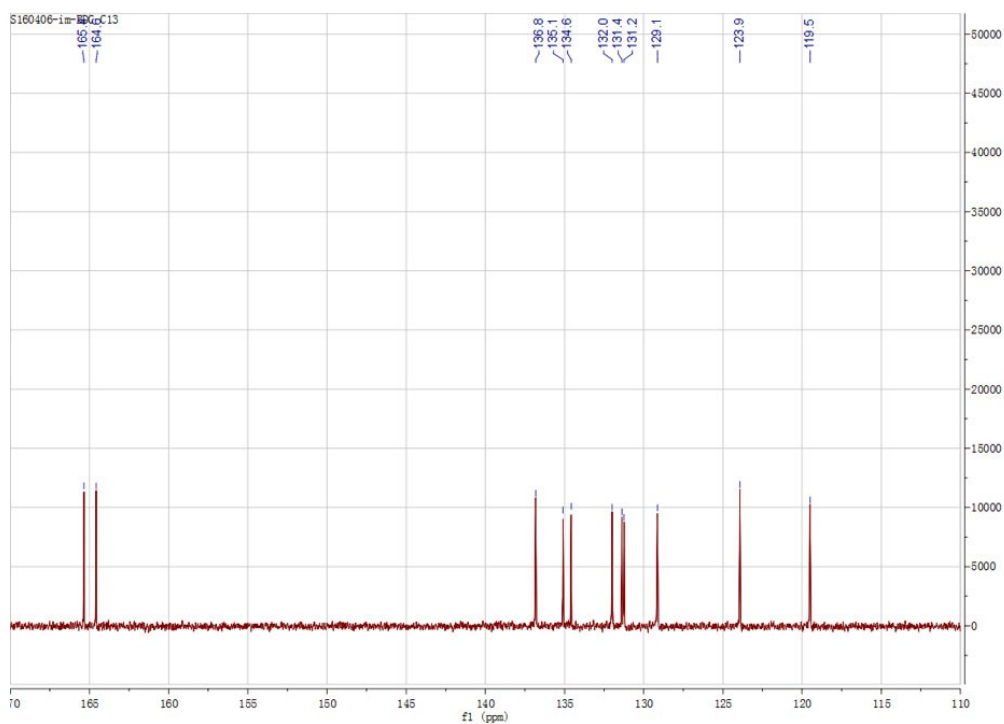


Fig. S3 ^{13}C NMR spectrum of $\text{Im-H}_2\text{BDC}\cdot\text{HCl}\cdot\text{H}_2\text{O}$ in $\text{DMSO-}d_6$ (r.t.).

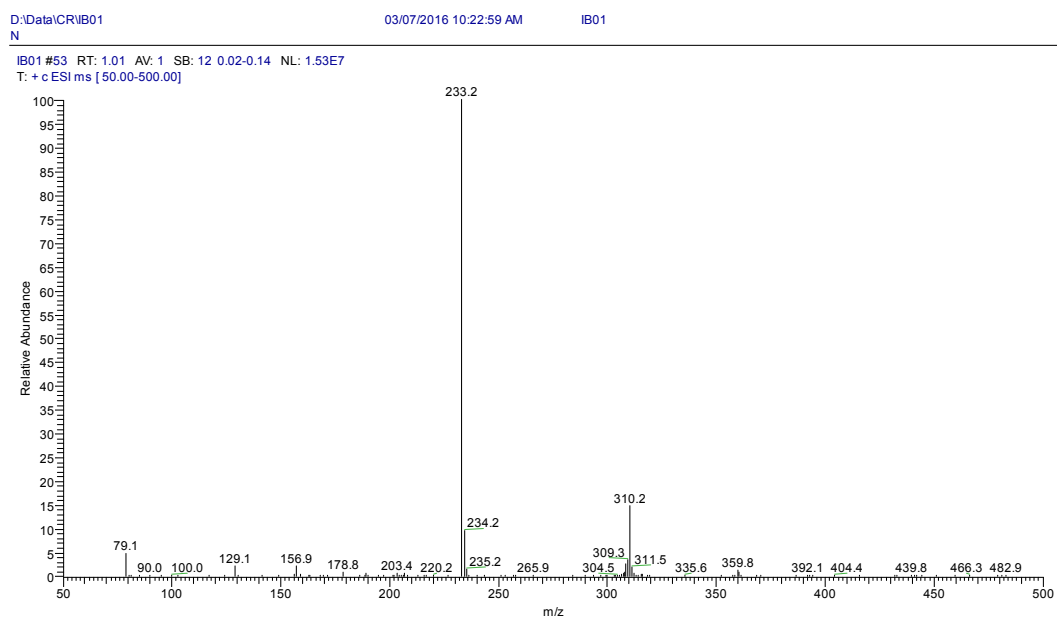


Fig. S4 The mass spectra of $\text{Im-H}_2\text{BDC}\cdot\text{HCl}\cdot\text{H}_2\text{O}$ in $\text{DMSO-}d_6$.

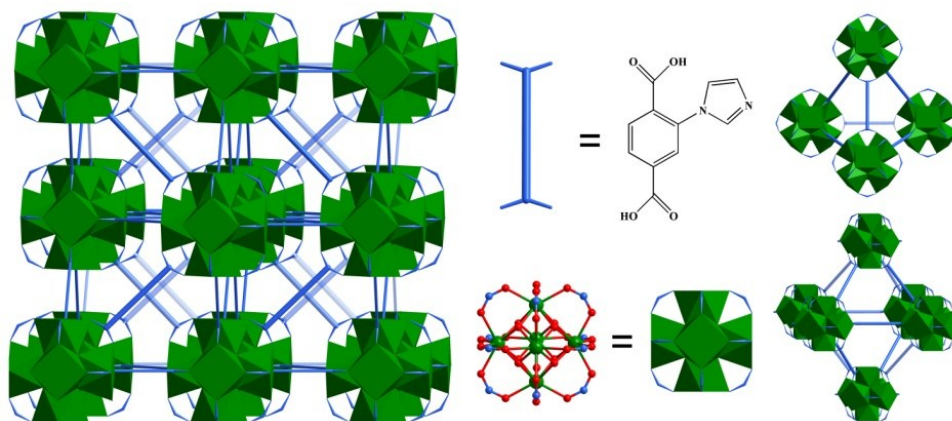


Fig. S5 Schematic view of Im-UiO-66 (**1**), composed of the six-centre octahedral metal cluster SBU, $[\text{Zr}_6(\text{OH})_4\text{O}_4(\text{CO}_2)_{12}]$ (green), and linear linkers (light blue), sustained by tetrahedral and octahedral cages. In the **fcu** topology, each cluster is connected to 12 neighboring clusters by im-BDC²⁻.

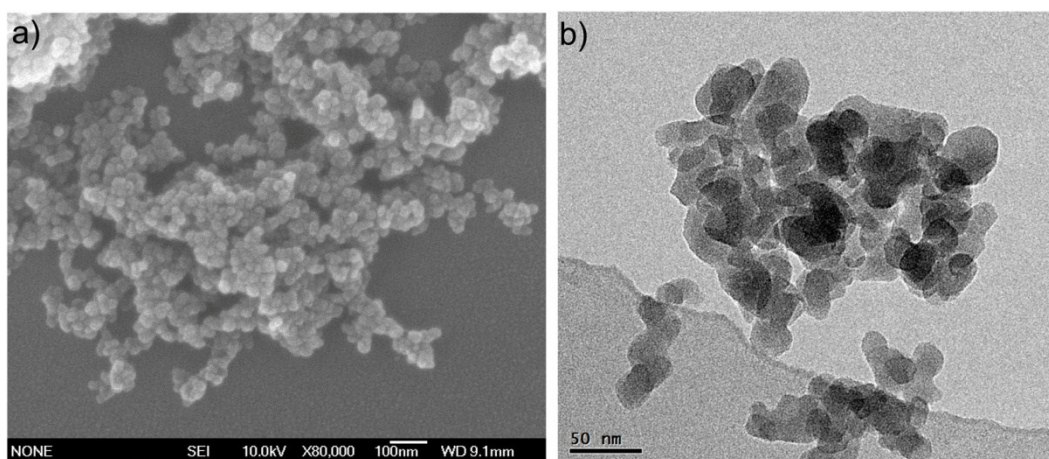


Fig. S6 a) The SEM and b) TEM spectra of as synthesized Im-UiO-66 (**1**) nanocrystals.

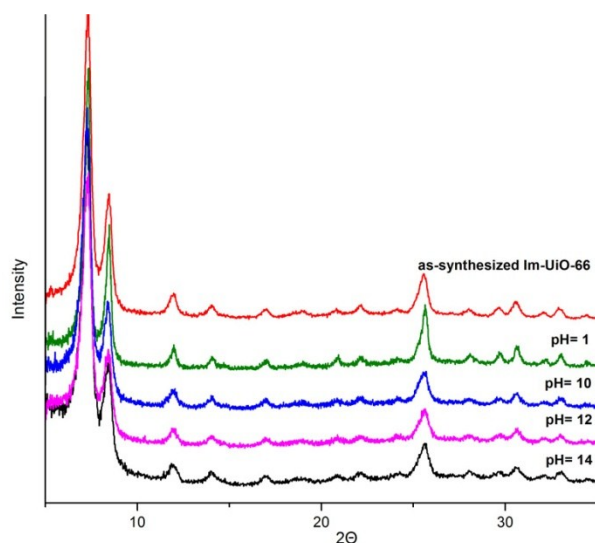


Fig. S7 Powder X-ray diffraction patterns of Im-UiO-66 (**1**) after being suspended in aqueous sodium hydroxide and hydrochloric conditions under specific pH value for 12 hours.

Table S1. Textural properties of MOFs in this work.

Sample	BET surface area (m^2g^{-1})	Total pore volume (cm^3g^{-1})	Pore diameter (nm)	CO_2 adsorption value (wt%)
1	538	1.11	0.7, 1.0, 1.3	5.85
2	328	0.88	0.6, 1.1	3.1
2 (after catalysis)	109	0.72	1.1	--
1 (NS)	560	0.43	0.6, 1.1, 3.4	5.5
2 (NS)	255	0.28	1.4, 1.8, 2.2, 3.0	3.26
UiO-66	803	0.62	0.6, 0.8, 1.0, 1.5	3.39

Note: The pore size distribution (PSD) profiles of **1**, **2**, **1** (NS), **2** (NS) and UiO-66 were based on Density functional theory method for micropores and Halsey standard method for mesopores, respectively. The pore diameter of **2** (after catalysis) was calculated by Horvath-Kawazoe method.

Analysis of CO₂-TPD and NH₃-TPD

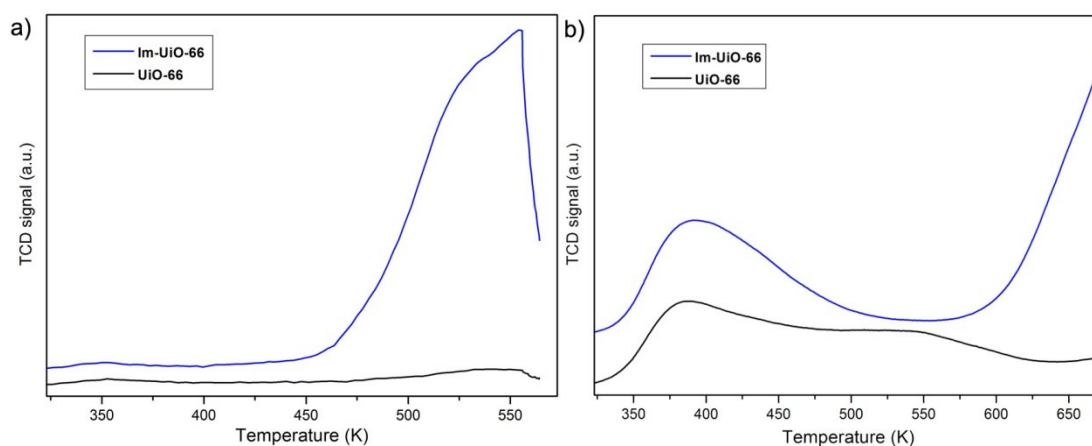


Fig. S8 (a) CO₂- and b) NH₃-TPD profiles of UiO-66 and Im-UiO-66 (**1**).

To understand the structural features of **1** more in detail, the acid–base characteristics of **UiO-66** and **1** were selectively examined using NH₃- and CO₂-TPD as shown in Figure S8. Jiang et al.² classified basicity in two groups: weak (323–450 K) and medium to strong (450–773 K). According to Figure S8a, CO₂-TPD measurement for **1** reveals the existence of medium Lewis basic sites with TPD peak around 525 K. In contrast, **UiO-66** presented much less but still some weak and medium basicity around 350 and 530 K, which was probably by the O atoms in the organic ligands connected to metal clusters.³ Figure S8b shows the NH₃-TPD profiles of **UiO-66** and **1**, and the distribution of the acidic sites in different strength was estimated following the guideline of Topsøe et al.: weak to medium (323–593 K) and strong (593–673 K).⁴ **UiO-66** showed weak to medium strength acidity, while **1** had weak to strong acidity, exhibiting two TPD peaks around 400 and 660 K. The (Zr-OH/Zr-OH₂) sites of defect Zr₆ clusters in **1** were expected to show some acidity.

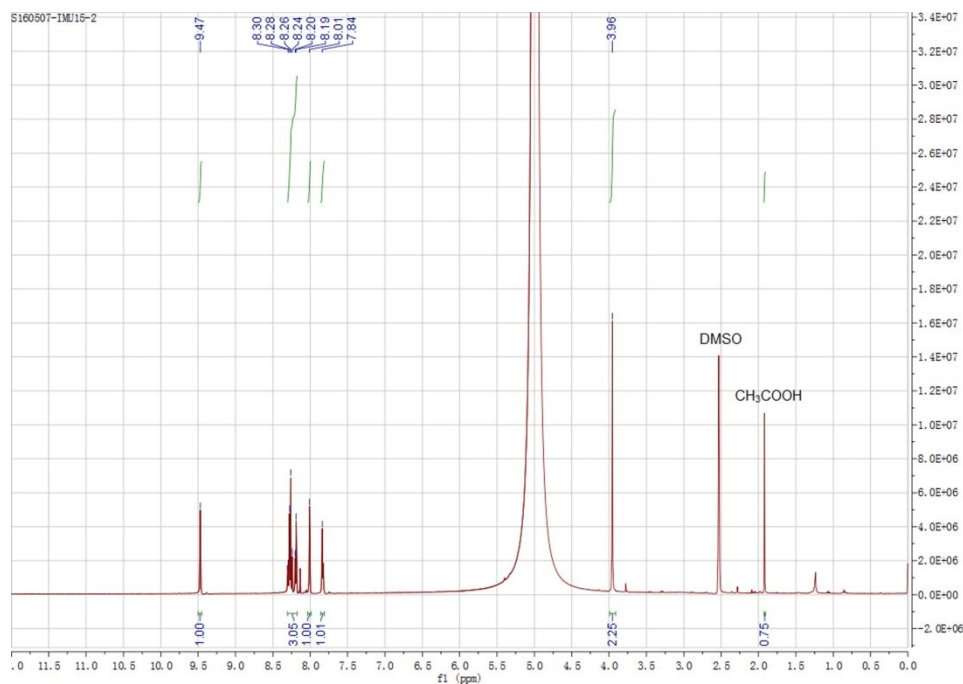


Fig. S9 ^1H NMR spectrum of digested (I)Meim-Uio-66 (**2**) sample in $\text{DMSO-}d_6$ (HF) (r.t).

The ^1H NMR spectrum of digested im-Uio-66 exhibited one set of expected signals attributed to im-BDC (not given). In contrast, the ^1H NMR spectrum of digested (I)Meim-Uio-66 showed a unique peak at 3.96 attributed to methyl group in Meim-BDC⁺.

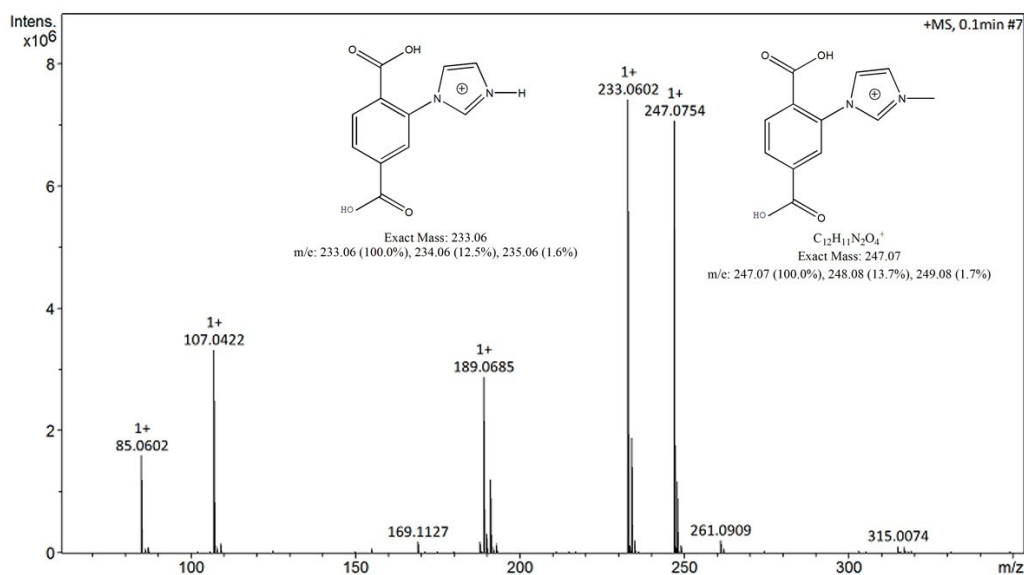


Fig. S10 The mass spectra of digested (I)Meim-Uio-66 (**2**) in $\text{DMSO-}d_6$ (HF)

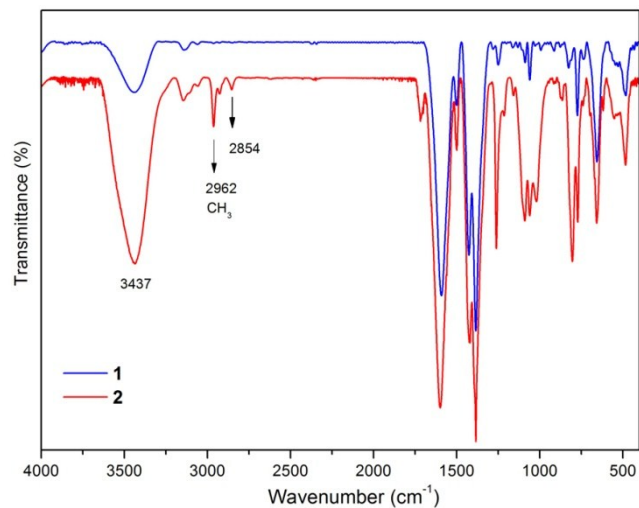


Fig. S11 The FT-IR spectra of Im-UiO-66 (**1**) and (I)Meim-UiO-66 (**2**).

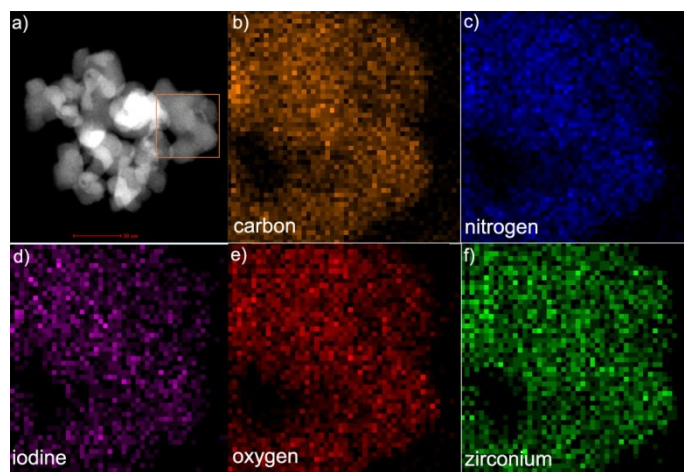


Fig. S12 a) HAADF-STEM image and b-f) corresponding element maps for **2**.

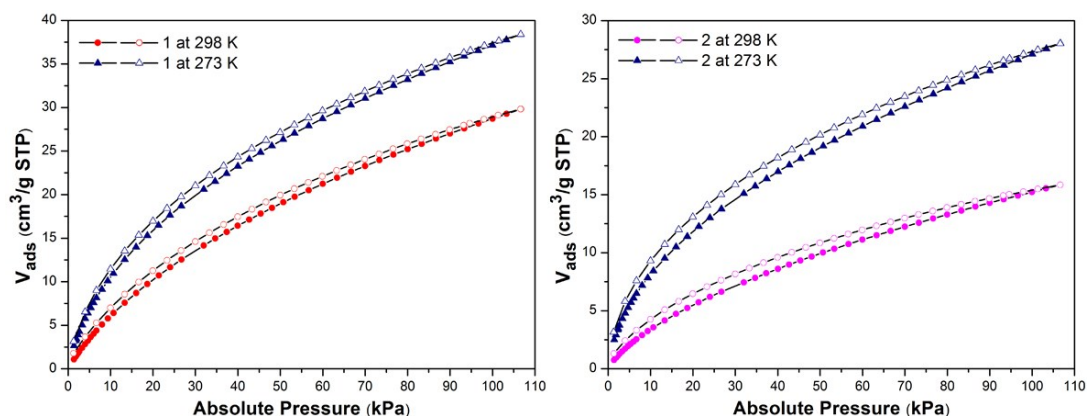


Fig. S13 CO₂ sorption isotherms for **1** and **2** at 273K and 298 K, respectively. Solid symbols denote adsorption, open symbols denote desorption.

Table S2. Zero-Coverage Heat of CO₂ adsorption in metal organic frameworks.

MOFs	Functionality type	-Q _{st} (kJ/mol)	Ref
Im-UiO-66(1)	imidazole	27.4	this work
MAF-7	--	17.2	5
MAF-26	--	23.3	5
MAF-4	--	25.1	5
MAF-25	--	26.3	5
MAF-2	--	27	6a
IFMC-1	--	30.7	5c
(I)Meim-UiO-66 (2)	imidazolium	44.2	this work
MOF-5	--	34	6a
UiO-66(Zr)-(COOH) ₂	carboxylic acid	34.8	6b
HKUST-1	exposed cations	35	6a
MOF-74-Ni	--	41.0	6b
Cu-TDPAT	--	42.2	6b
Bio-MOF-11	--	45.0	6b
MOF-74-Mg	exposed cations	47	6a
TBA@bio-MOF-1	amines	55	6a

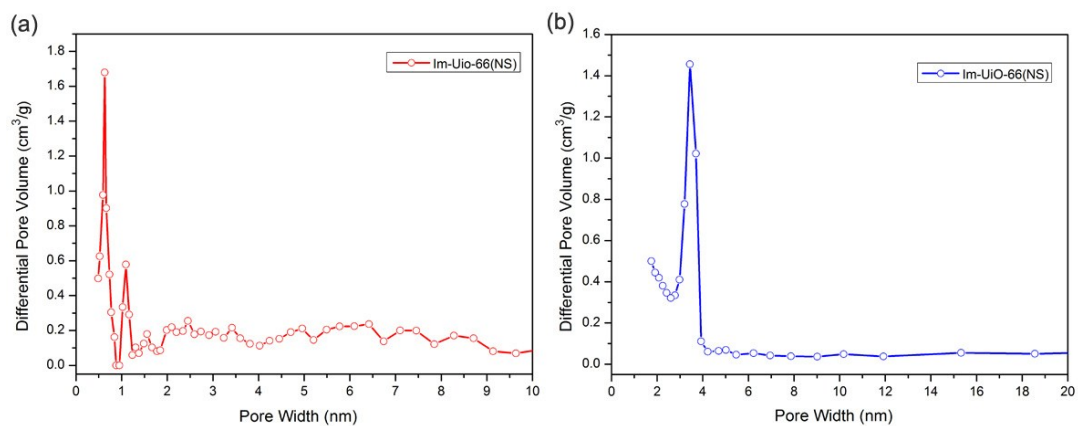


Fig. S14 The pore size distribution (PSD) profiles of **1** (NS) based on Density functional theory method for micropores (6 Å and 11 Å) and Halsey standard method for mesopores (centered at 34 Å), respectively.

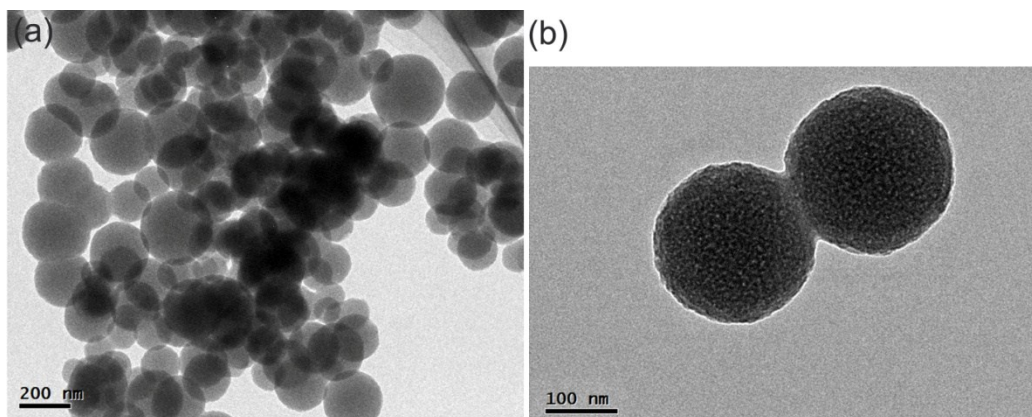


Fig. S15 HRTEM images of Zr-MOF nanospheres **1** (NS).

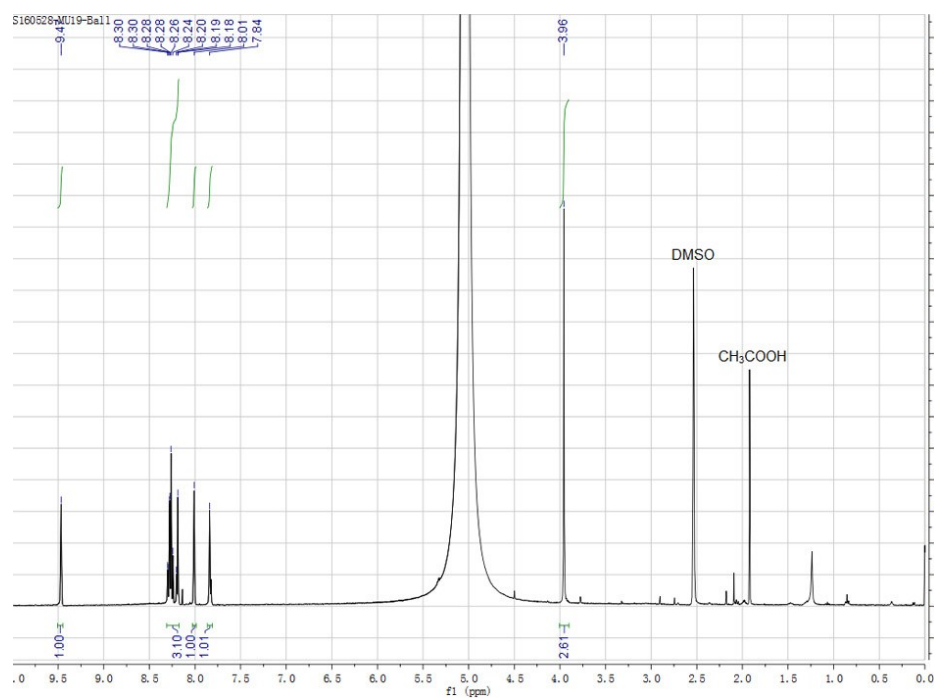


Fig. S16 ^1H NMR spectrum of digested **2** (NS) sample in $\text{DMSO-}d_6$ (HF) (r.t).

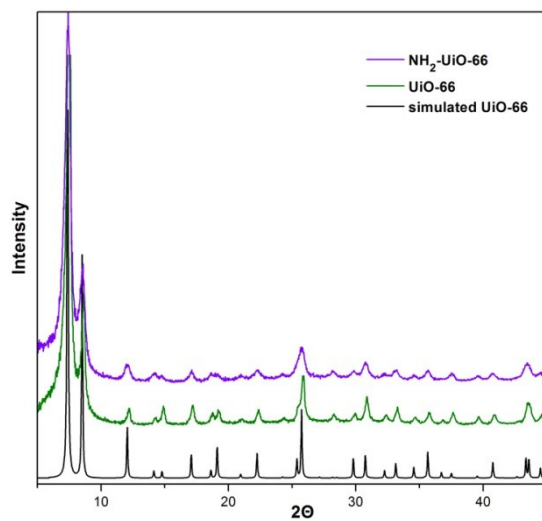


Fig. S17 Powder X-ray diffraction patterns of as-synthesized UiO-66 and NH_2 -UiO-66.

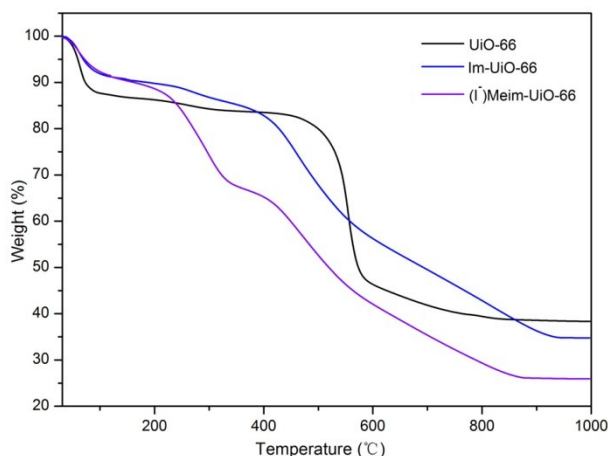


Fig. S18 Thermo gravimetric curves of (a) UiO-66, (b) Im-UiO-66, and (c) (I)Meim-UiO-66.

Both Im-Uio-66 (**1**) and (I)Meim-Uio-66 (**2**) exhibit three characteristic weight losses, however, the thermal stability of Im-UiO-66 seems to be better than that of (I)Meim-UiO-66. For Im-UiO-66: first the departure of the guest molecules (H_2O) between 30 °C and 100 °C (8 %) and second the departure of free acid still remaining in the pores between 100 and 400 °C (9 %). The third weight loss, between 400 and 900 °C, corresponds to the degradation of the framework (48%). For (I)Meim-UiO-66: first the departure of the guest molecules (H_2O) between 25 and 100 °C (8 %) and second the departure of free acid still remaining in the pores between 100 and 200 °C (4 %). After that, the framework decomposed rapidly until 880 °C (62%).

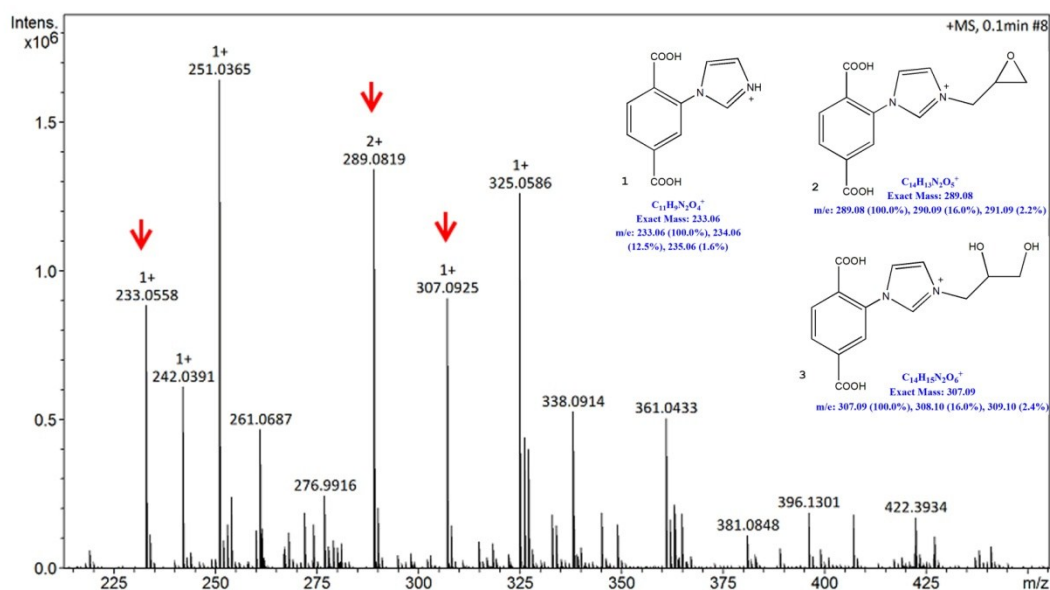


Fig. S19 The mass spectra of digested **1** (after catalysis) in DMSO-*d*₆ (HF). It revealed that more than two Im-BDC derivatives had formed in the generated ionic catalyst during the catalysis process.

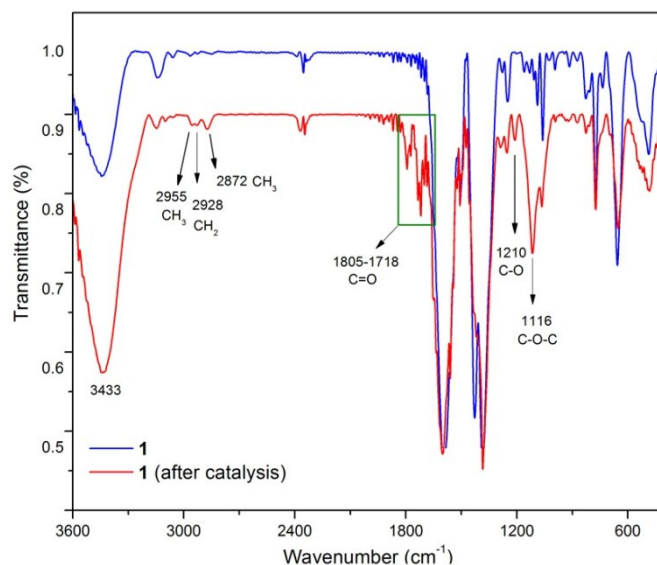
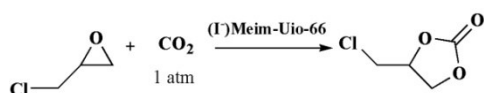


Fig. S20 The FT-IR spectra of Im-Uio-66 (**1**) before and after catalysis.

4. Catalysis

Table S3. Cycloaddition of CO₂ with epichlorohydrin catalyzed by **2**.^[a]



Entry	Temp (°C)	Time (h)	Conversion ^[b] (%)	Yield	Selectivity ^[b] (%)	TON (%)
1	100	24	88.5	85.1	94.3	114
2	110	24	97.0	92.0	94.9	123
3	115	24	98.4	92.9	94.4	124

4	120	12	89.5	83.5	93.3	112
5	120	18	95.8	88.8	92.7	119
6	120	24	100	93.6	93.6	125

[a] Reaction condition: epoxides 10 mmol, **2** (0.05 g, 0.745 mol%), 0.1 MPa of CO₂ pressure. [b] Determined by GC-MS. [c] Turnover number (product (mmol)/imidazolium (mmol)).

Table S4. The cycloaddition of CO₂ and epichlorohydrin using different catalysts .^[a]

Entry	Catalyst	Conversion ^[b] (%)	Yield (%)	Selectivity ^[b] (%)
1	2	100	93.6	93.6
2	2 (NS)	66	59	90
3	UiO-66	trace	trace	n.d
4	NH ₂ -UiO-66	11	6.4	57
5	H ₂ BDC	0	0	n.d
6	Im-H ₂ BDC + ZrCl ₄	100	38.5	38.5

[a] Reaction condition: 10 mmol of epichlorohydrin at 393 K, 24 h and 0.1 MPa of CO₂ pressure using 50 mg of catalyst components each. [b] Determined by GC-MS. H₂BDC: terephthalic acid.

Table S5. The cycloaddition of CO₂ with epoxides catalized by different catalysts.^[a]

Entry	Substrate	Catalyst.	Conversion. ^[b] (%)	Selectivity ^[b] (%)
1	Styrene oxide	2	46	71
2	Styrene oxide	1	4.0	34
3	1,2-epoxyhexane	2	61	38
4	1,2-epoxyhexane ^c	2	37	n.d
5	1,2-epoxyhexane	1	14	69

[a] Reaction conditions: 10 mmol of epoxide at 393 K and 0.1 MPa of CO₂ pressure using 50 mg of catalyst each, 24h. [b] Determined by GC-MS. [c] In closed air atmosphere.

Table S6. Recycled experiments of cycloaddition of CO₂ with epichlorohydrin catalyzed by **2**.^[a]

Run	Conversion. ^[b] (%)	Yield (%)	Selectivity ^[b] (%)
1	100	93.6	93.6
2	98.5	92.4	93.8
3	99.5	92.4	93.0
4	97.9	90.8	92.7
5	99.3	93.7	94.4
6	99.0	95.5	96.5

[a] Reaction conditions: epoxides 10 mmol, catalyst 0.05 g, P_{CO₂} (0.1MPa), Temperature (120°C), Time (24h). [b] Determined by GC-MS.

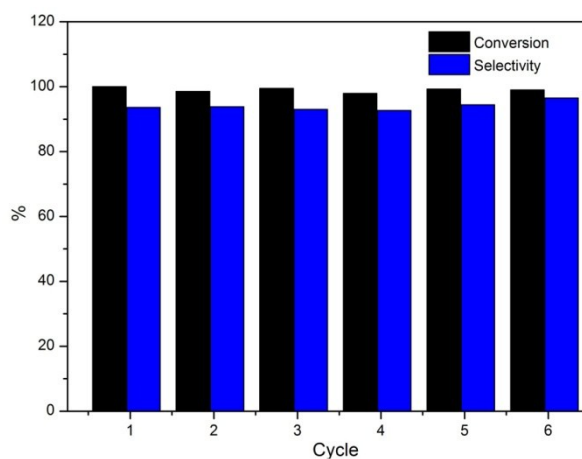


Fig. S21 Recycled experiments of **2**.

5. References

- 1 K. H. Cui, S. Y. Yao, H. Q. Li, Y. T. Li, H. P. Zhao, C. J. Jiang and Y. Q. Tian, *CrystEngComm.*, 2011, **13**, 3432.
- 2 G. Jiang, L. Zhang, Z. Zhao, X. Zhou, A. Duan, C. Xu, J. Gao, *Appl. Catal. A: Gen.*, 2008, **340**, 176.
- 3 J. Kim, S. N. Kim, H. G. Jang, G. Seo, W. S. Ahn, *Applied Catalysis A: General.*, 2013, **453**, 175.
- 4 N. Y. Topsøe, K. Pedersen, E. G. Derouane, *J. Catal.*, 1981, **70**, 41.
- 5 (a) J.-P. Zhang, A.-X. Zhu, R.-B. Lin, X.-L. Qi and X.-M. Chen, *Adv. Mater.*, 2011, **23**, 1268–1271; (b) J.-B. Lin, J.-P. Zhang and X.-M. Chen, *J. Am. Chem. Soc.*, 2010, **132**, 6654–6656; (c) J. S. Qin, D. Y. Du, W. L. Li, J. P. Zhang, S. L. Li, Z. M. Su, X. L. Wang, Q. Xu, K.Z. Shao, Y. Q. Lan, *Chem. Sci.*, 2012, **3**, 2114.
- 6 (a) K. Sumida, D. L. Rogow, J. A. Mason, T. M. McDonald, E. D. Bloch, Z. R. Herm, T. H. Bae, and J. R. Long, *Chem. Rev.*, 2012, **112**, 724; (b) Q. Yang, S. Vaesen, F. Ragon, A. D. Wiersum, D. Wu, A. Lago, T. Devic, C. Matineau, F. Taulelle, P. L. Llewellyn, H. Jobic, C. Zhong, C. Serre, G. D. Weireld, G. Maurin, *Angew. Chem. Int. Ed.*, 2013, **52**, 1.